J. Fluid Mech. (1979), *vol.* 92, *part* 4, *pp.* 767–781
Printed in Great Britain

Nonlinear water waves generated by an accelerated circular cylinder

By H. J. HAUSSLING AND R. M. COLEMAN

David W. Taylor Naval Ship Research and Development Center,
Bethesda, Maryland 20084

(Received 24 July 1978 and in revised form 31 October 1978)

Numerical solutions for the irrotational flow of an incompressible fluid about a circular cylinder accelerated from rest below a free surface are presented. The usual restriction to linearized free-surface boundary conditions has been avoided. The transient period from the start to a local steady state or to the development of a very steep wave slope is investigated in terms of free-surface profiles and body-surface pressure distributions. Linear and nonlinear results are used to illustrate the transition from deep submergence when nonlinear effects are small to shallow submergence when linearized analysis is inaccurate.

1. Introduction

The time-dependent irrotational flow of an incompressible fluid past a circular cylinder accelerated from rest below a free surface has been analysed by numerical methods. A paper presented at the Second International Conference on Numerical Ship Hydrodynamics (Haussling & Coleman 1977) described the procedure used and presented some initial results. The work reported in that paper revealed two basic results. (1) When the method was applied to the linearized equations the computed flow evolved toward a steady state which showed excellent agreement with linearized steady-state results obtained by other methods. (2) When the method was applied to the nonlinear problem for shallow submergence the flow evolved until a very steep wave slope developed downstream from the cylinder. The nonlinear development could not be pursued beyond this point because of limitations in the mathematical model. Thus no nonlinear steady state was achieved.

In more recent work nonlinear steady-state solutions have been found. For intermediate submergence the flow evolves toward a steady state which differs from the linearized steady state. Even for shallow submergence a nonlinear steady state is achieved through the application of a free-surface pressure distribution to prevent (or simulate) wave breaking. The present paper uses these new results to give a picture of the effect of the depth of submergence on both the linear and nonlinear flows. For deep submergence nonlinear effects are of limited significance; and for shallow submergence linearized analysis is inaccurate.

Various investigators have previously considered the problem of determining the flow about, and the pressure distribution on, a submerged body in motion relative to a fluid having a free surface. The situation in which the body is a circular cylinder has frequently been considered as a test problem for different methods because it retains

0022-1120/79/4265-6790 $02.00

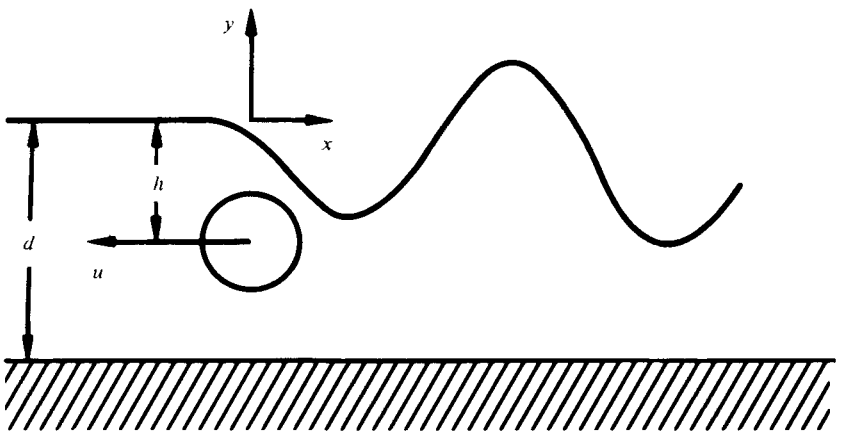

FIGURE 1. Circular cylinder at submergence depth h moving through water of depth d.

the free-surface features while eliminating the difficulties of treating a more complicated body shape. Havelock (1936) obtained a steady-state analytic solution for a circular cylinder translating horizontally at constant speed below a free surface. Giesing & Smith (1967) solved the same problem by a numerical solution of an integral equation obtained through the use of a Green's function. More recently the finite-element method has been successfully tested on this problem (Bai 1975; Mei & Chen 1976; Zarda & Marcus 1977).

In all of this previous work the free-surface boundary conditions were linearized. In the present study this restriction has been dropped. Because it is not known in advance whether a particular nonlinear problem will have a steady-state solution, the unsteady problem has been considered.

2. The flow problem

The flow development due to the acceleration from rest of a circular cylinder of infinite span in an incompressible fluid bounded above by a free surface and below by a rigid wall is considered. The fluid is initially at rest and has uniform depth d as defined in figure 1. The depth of submergence (the distance from the undisturbed free surface to the centre of the cylinder) is h and the horizontal speed of the cylinder is u. An (x, y) co-ordinate system moves with the body and has its origin located at the level of the undisturbed free surface. It is assumed that the flow is irrotational and that the fluid is incompressible and lacks surface tension. It is also assumed that the surface elevation can be described at any time t by specifying y as a single-valued function of x: $y = Y(x, t)$. This assumption is not valid if the waves approach breaking conditions. In such a case a more sophisticated formulation would be necessary.

The dimensionless form of the initial/boundary-value problem in the moving reference frame for the free-surface elevation Y and potential ϕ for the velocity relative to a frame at rest is

$$\phi_{xx}+\phi_{yy} = 0 \quad -\infty < x < \infty, \quad -d < y < Y; \tag{1}$$

$$Y_t = (u(t)-\phi_x)Y_x+\phi_y \quad \text{at} \quad y = Y; \tag{2}$$

$$\phi_t = u(t)\,\phi_x - Y/Fr^2 - \tfrac{1}{2}(\phi_x^2+\phi_y^2) \quad \text{at} \quad y = Y; \tag{3}$$

$$\nabla\phi\cdot\hat{\mathbf{n}} = \begin{cases} 0 & \text{at} \quad y = -d, \\ -u\hat{\mathbf{i}}\cdot\hat{\mathbf{n}} & \text{at the body surface;} \end{cases} \tag{4}$$

$$\phi_x = 0 \quad \text{at} \quad x = \pm\infty; \tag{5}$$

$$\phi = 0, \quad Y = 0 \quad \text{at} \quad t = 0. \tag{6}$$

The subscripts x, y and t denote differentiation. The characteristic length and velocity scales in the dimensionless quantities are D, the diameter of the cylinder, and U, its final speed. The Froude number is $Fr = U/(gD)^{\frac{1}{2}}$, where g is the gravitational acceleration. The unit normal vector to a boundary is $\hat{\mathbf{n}}$, and $\hat{\mathbf{i}}$ is a unit vector in the x direction. The pressure at the free surface is denoted by p_s.

The dynamic pressure p on the body surface can be computed from the Bernoulli equation

$$p = -\phi_t + u\phi_x - \tfrac{1}{2}(\phi_x^2+\phi_y^2). \tag{7}$$

The resistance and lift coefficients are

$$R = \text{resistance}/\rho DU^2 = -\int p\hat{\mathbf{n}}\cdot\hat{\mathbf{i}}\,ds \tag{8}$$

and

$$L = \text{lift}/\rho DU^2 = \int p\hat{\mathbf{n}}\,.\,\hat{\mathbf{j}}\,ds, \tag{9}$$

where $\hat{\mathbf{j}}$ is a unit vector in the y direction, and where the integrations are over the body surface.

In all cases the cylinder accelerates uniformly from rest to its final speed during one unit of dimensionless time. That is

$$u = \begin{cases} 0 & t \leqslant 0, \\ t & 0 < t \leqslant 1, \\ 1 & 1 < t. \end{cases} \tag{10}$$

In all cases but one the pressure at the free surface is specified to be zero ($p_s = 0$). In the one exceptional case the effect of a locally non-zero surface pressure on the developing flow is investigated.

3. Method of solution

This section presents an outline of the numerical method used to solve the initial/boundary-value flow problem. Details can be found in the previous paper by the authors (Haussling & Coleman 1977).

To simplify the numerical solution of the problem, the time-dependent physical region in (x, y) space (figure 1), cut off suitably far upstream and downstream, is transformed to a time-independent computational region in (ξ, η) space which, as shown in figure 2, is composed solely of rectangles. The cylinder is mapped onto the slit LE, the free-surface onto AB, the bottom of the water onto IH, the upstream boundary onto AN and JI, and the downstream boundary onto BC and GH. The boundaries $JKLMN$ and $CDEFG$ represent cuts within the fluid.

The desired transformation represented by

$$\xi = \xi(x, y, t) \quad \text{and} \quad \eta = \eta(x, y, t) \tag{11}$$

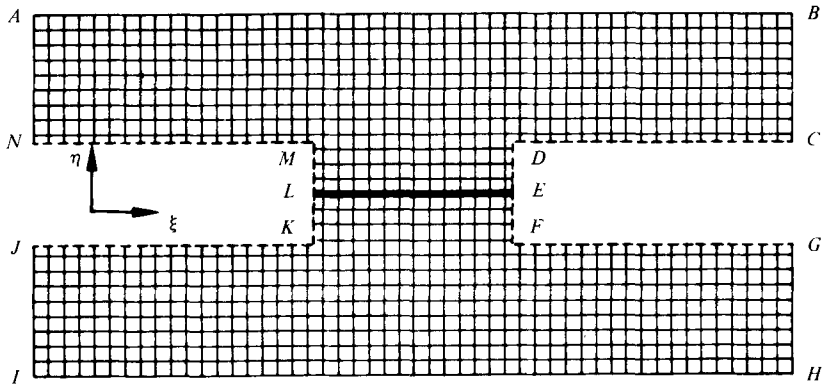

FIGURE 2. The computational region and co-ordinate system.

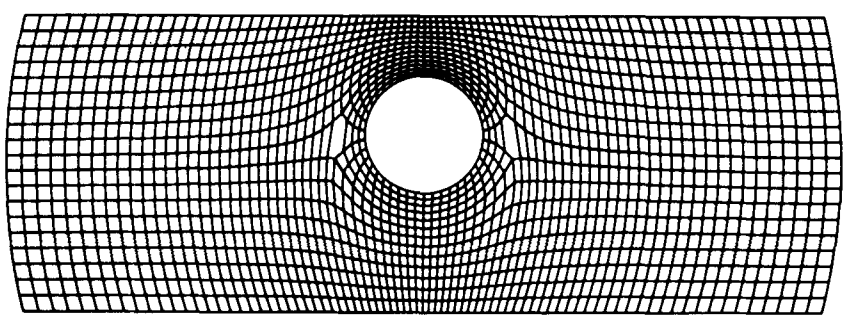

FIGURE 3. The computational co-ordinate system in physical space at $t = 0$.

is computed using methods employed by Thames *et al.* (1977) to generate similar mappings. The transformations are required to be solutions of Poisson equations

$$\xi_{xx} + \xi_{yy} = P(\xi, \eta, t) \tag{12}$$

and

$$\eta_{xx} + \eta_{yy} = Q(\xi, \eta, t), \tag{13}$$

subject to appropriate boundary conditions. The source functions P and Q are specified such that the resulting (ξ, η) co-ordinate system is suitable for the numerical calculations.

For computational purposes, the generating system (12) and (13) and the flow problem (1)–(6) are transformed to the (ξ, η) space. Thus the flow problem is solved using a time-dependent (ξ, η) co-ordinate system which at $t = 0$, when the water is undisturbed, appears as in figure 3. The co-ordinate system is cylindrical near the body but also conforms to whatever region is occupied by the water.

Both the transformation and flow problems are solved numerically. The domain of integration in the (ξ, η) plane is replaced by a uniform network of grid points (figure 2). The differential equations are replaced by difference equations involving the values of the dependent variables at these grid points. The finite difference versions of the transformed potential equation and transformation generation equations are solved using successive over-relaxation.

Euler's modified method of time differencing is used to replace the transformed versions of the free-surface boundary conditions (2) and (3) with a suitable implicit

Cylinder submergence h	Water depth d	Free-surface boundary conditions
1·0	2·5	Linearized and nonlinear
2·0	4·0	Nonlinear
1·5	3·0	Linearized and nonlinear
1·25	2·75	Nonlinear

TABLE 1. The various cases considered. In all cases $Fr = 0{\cdot}566$. Each case is referred to by its depth of submergence h.

marching scheme. The marching equations along with the potential and transformation generation equations are solved in a combined iterative procedure.

A numerical filtering scheme was introduced to eliminate the instability which is usually present in such marching methods for nonlinear water wave problems. Filtering techniques were discussed by Shapiro (1975) and used successfully by Longuet-Higgins & Cokelet (1976) to eliminate such a numerical instability encountered in the calculation of the development of breaking waves.

In all cases considered the upstream and downstream computational boundaries were located a distance of about 11 diameters from the body. Grid systems were used with about 3000 points having configurations near the body similar to that shown in figure 3. Storage occupied about 60000 words on a CDC 6400 computer. With a time step of 0·03 about 90 min of CDC 6400 CPU time was needed to calculate the flow development for a non-linear case to almost steady state in the neighbourhood of the cylinder.

4. Results

The cases considered are listed in table 1 in the order in which they will be discussed.

4.1. $h = 1{\cdot}0$

The linearized version of the problem was considered first to test the numerical method on a case for which there was a pre-existing steady-state solution for comparison. The nonlinear terms were omitted from the free-surface boundary conditions and those conditions were applied at the level of the undisturbed free surface. The results, which were presented in Haussling & Coleman (1977), showed that the unsteady numerical solution approached asymptotically the steady-state results of Giesing & Smith (1967) for both the forces on the cylinder and the free-surface elevation. In the steady-state solution the free surface was essentially tangent to the body surface, a configuration indicating that the linear solution was far from reality.

In considering this submergence, $h = 1{\cdot}0$, with the exact boundary conditions, the solution could be pursued for only a short time, until about $t = 0{\cdot}8$ by which point a very large velocity gradient had developed above the cylinder. The inability to continue the solution beyond this time indicates a deficiency in either the mathematical or numerical model in such a highly nonlinear case.

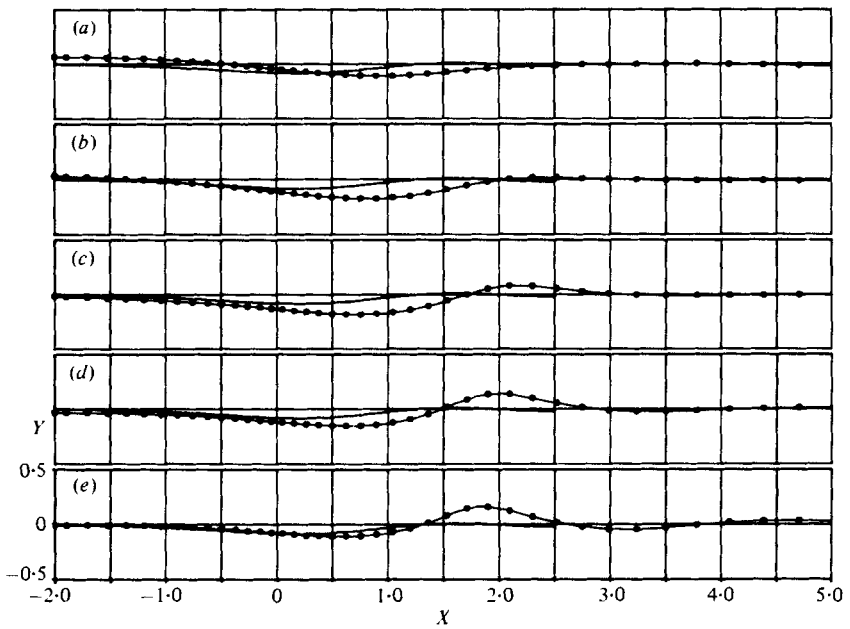

FIGURE 4. Nonlinear free-surface evolution compared with the linear steady-state solution: $h = 2$, $d = 4$. —●—, unsteady; ——, steady state. (*a*) $t = 3{\cdot}0$. (*b*) $t = 4{\cdot}5$. (*c*) $t = 6{\cdot}0$. (*d*) $t = 7{\cdot}5$. (*e*) $t = 9{\cdot}0$.

4.2. $h = 2{\cdot}0$

In figure 4 the development of the free-surface elevation is compared with the linear steady-state solution obtained using the NASTRAN finite-element programme according to the technique of Zarda & Marcus (1977). The initial flow development is quite linear. However, the surface elevation approaches a steady state which is somewhat different from the linear result. At $t = 9$, when the flow is at almost steady state near the body, the linear and non-linear surface elevations, which are shown in detail in figure 5, deviate significantly downstream from $x = 0$. The nonlinear elevation continues to drop with increasing x to about $x = 0{\cdot}5$ and then rises abruptly to a high peak near $x = 1{\cdot}8$. The maximum slope on the upstream face of the wave is

$$dY/dx \simeq 0{\cdot}38.$$

This compares with the largest non-breaking wave slope $dY/dx \simeq 0{\cdot}47$ found in experiments by Salvesen & von Kerczek (see the discussion of Haussling & Coleman, 1977). This difference between the linear and nonlinear results occurs in spite of the facts that the linear wave slopes are quite small and that the reduction of the gap between the water surface and the cylinder is less than 10% of the undisturbed gap.

In figures 6 and 7 are plotted the various terms in the free-surface boundary conditions. Figure 6 shows that the nonlinear terms in the dynamic free-surface boundary condition, while smaller in absolute value than the linear terms, are by no means negligible. As one approaches the waves from upstream, substantial values of ϕ_x^2 are first encountered between $x = -0{\cdot}5$ and $x = 0$. Between $x = 0{\cdot}5$ and $1{\cdot}0$ ϕ_y^2 becomes significant. Although the nonlinear term $\phi_x Y_x$ in the kinematic free-surface condition is also significant (figure 7), the rapid rise in the surface downstream from the body is not associated directly with this term but rather with large values of ϕ_y in this region.

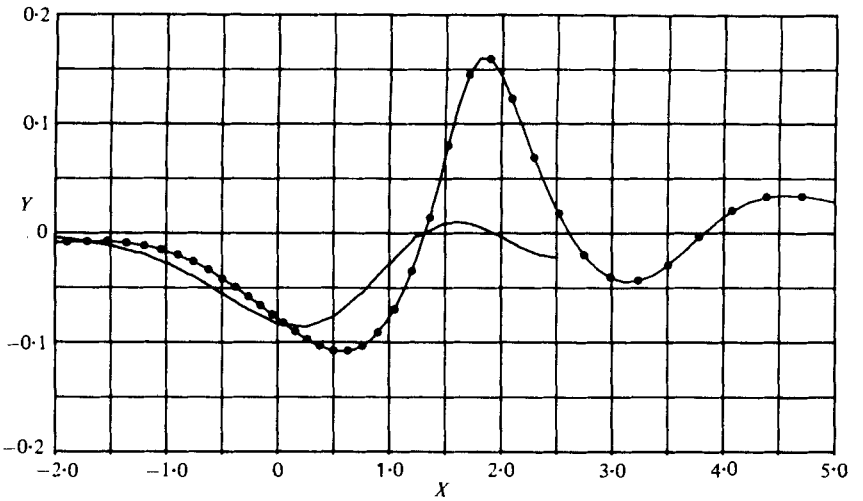

FIGURE 5. Detail from figure 4 showing the nonlinear free surface at $t = 9$ and the linear steady-state profile. —●—, nonlinear; ——, linear.

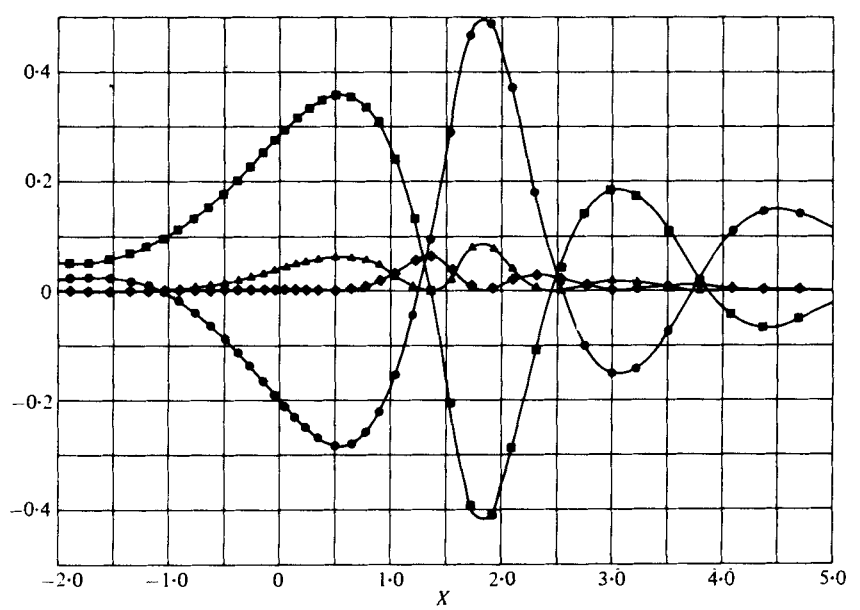

FIGURE 6. The terms in the dynamic free-surface boundary condition (3) plotted *vs.* x at $t = 9{\cdot}6$ for $h = 2$ and $d = 4$. —■—, ϕ_x; —▲—, $\frac{1}{2}\phi_x^2$; —◆—, $\frac{1}{2}\phi_y^2$; —●—, Y/Fr^2X.

Although the linear and nonlinear surface elevations are significantly different, there is quite good agreement between the corresponding body pressure distributions as shown in figure 8. The nonlinear pressure at $t = 9{\cdot}6$ is somewhat greater in absolute value than the linear pressure, particularly on the upper surface. This small difference is due to the application of the nonlinear boundary conditions at the actual free-surface location which is closer to the body than it is in the undisturbed position. The water passes through this reduced gap with higher speed than it would need to pass through the undisturbed gap.

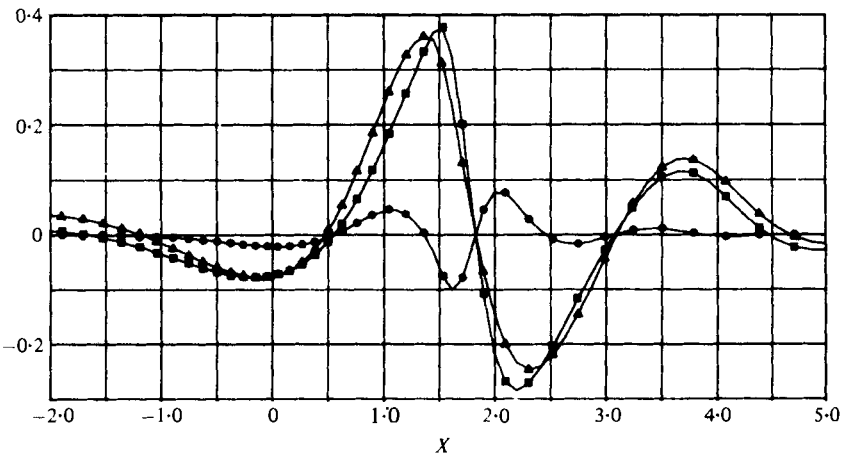

FIGURE 7. The terms in the kinematic free-surface boundary condition (2) plotted *vs.* x at $t = 9{\cdot}6$ for $h = 2$ and $d = 4$. —▲—, ϕ_y; —■—, Y_x; —●—, $\phi_x Y_x$.

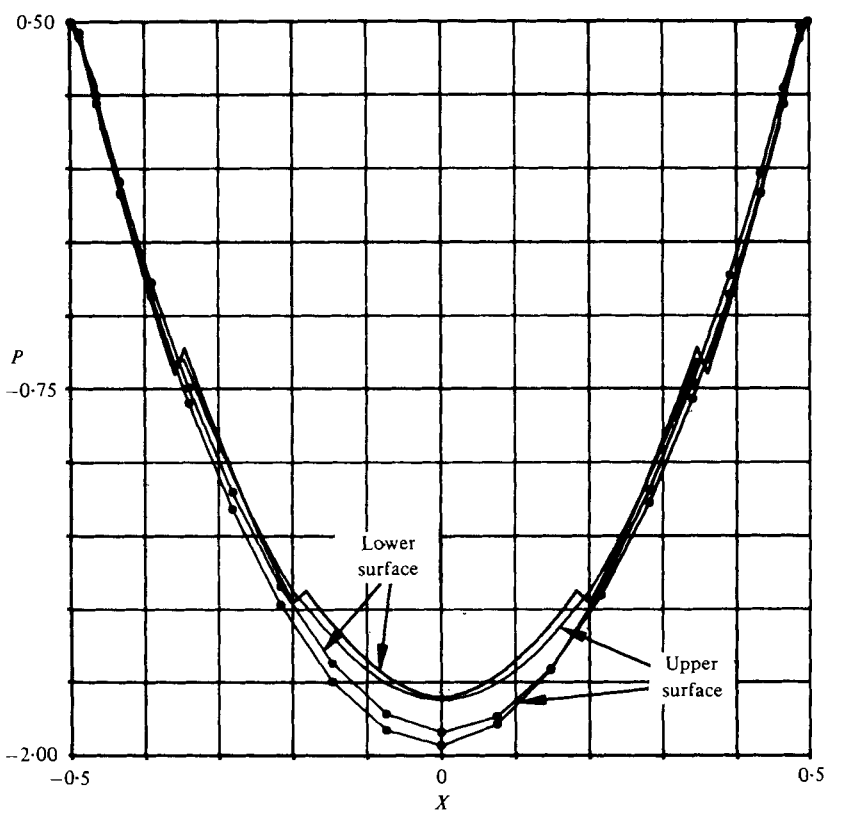

FIGURE 8. The dynamic pressure on the body surface at $t = 9{\cdot}6$ compared with the linear steady-state pressure: $h = 2$, $d = 4$. —●—, nonlinear; ——, linear.

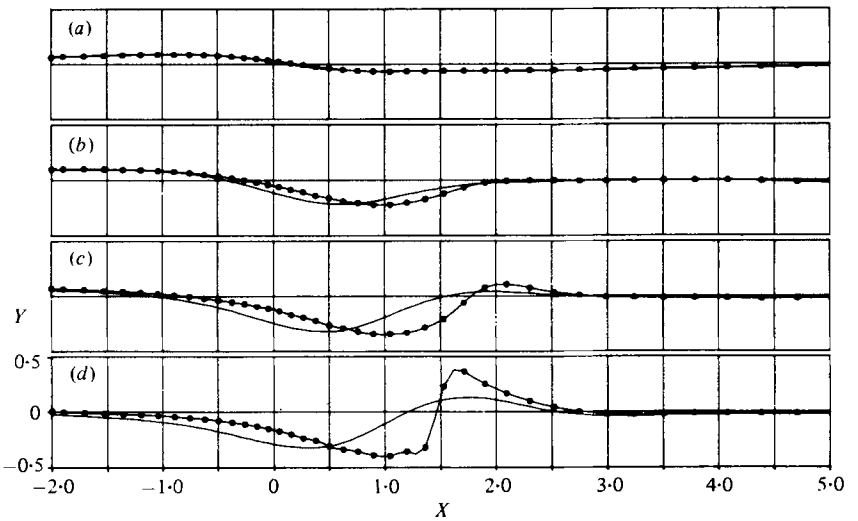

FIGURE 9. Linear and nonlinear free-surface evolution for $h = 1{\cdot}5$ and $d = 3$. ——, linear; —●—, nonlinear. (*a*) $t = 1{\cdot}5$. (*b*) $t = 3{\cdot}0$. (*c*) $t = 4{\cdot}5$. (*d*) $t = 6{\cdot}0$.

4.3. $h = 1{\cdot}5$

The free-surface evolutions for the linear and nonlinear problems are compared in figure 9. In the early development, when wave slopes are small, the two cases are essentially identical. At later times there are substantial differences. The nonlinear development is similar to that for $h = 2{\cdot}0$ to $t = 4{\cdot}5$, except that for $h = 1{\cdot}5$ the surface displacements and slopes are considerably greater. By $t = 6{\cdot}0$ a very steep slope $dY/dx \simeq 3{\cdot}5$ has developed at about $x = 1{\cdot}5$. The wave appears to be well on its way to breaking conditions. Unfortunately, the calculations cannot be carried out beyond this time because of the limitations of the mathematical/numerical model. The assumption of a single-valued free surface means that accuracy deteriorates as the surface slope increases. In fact, the calculations break down shortly after $t = 6{\cdot}0$. The deterioration of the solution is already visible at $t = 6{\cdot}0$ in the form of free-surface oscillations in the trough between $x = 1$ and $1{\cdot}5$. With an improved surface representation, the calculations might be continued somewhat farther into the breaking process, as was done by Longuet-Higgins & Cokelet (1976).

The overall flow development is shown by the streamlines in figure 10. When the surface is steady, the streamlines are parallel to it. In figure 10(*d*) the streamlines interesecting the surface indicate that the surface is changing rapidly.

The use of a surface pressure distribution to inhibit the development of such a breaking wave was investigated. The pressure was assigned the form

$$p_s(x,t) = \begin{cases} \phi_n(Y_x - 1)^2 & Y_x > 1, \\ 0 & \text{otherwise.} \end{cases} \tag{14}$$

This pressure is thus automatically applied whenever the surface slope exceeds unity. Because the pressure is proportional to ϕ_n, the velocity normal to the free surface (positive away from the water), it always performs negative work on the fluid and therefore removes energy from the flow. Such a pressure distribution can be viewed

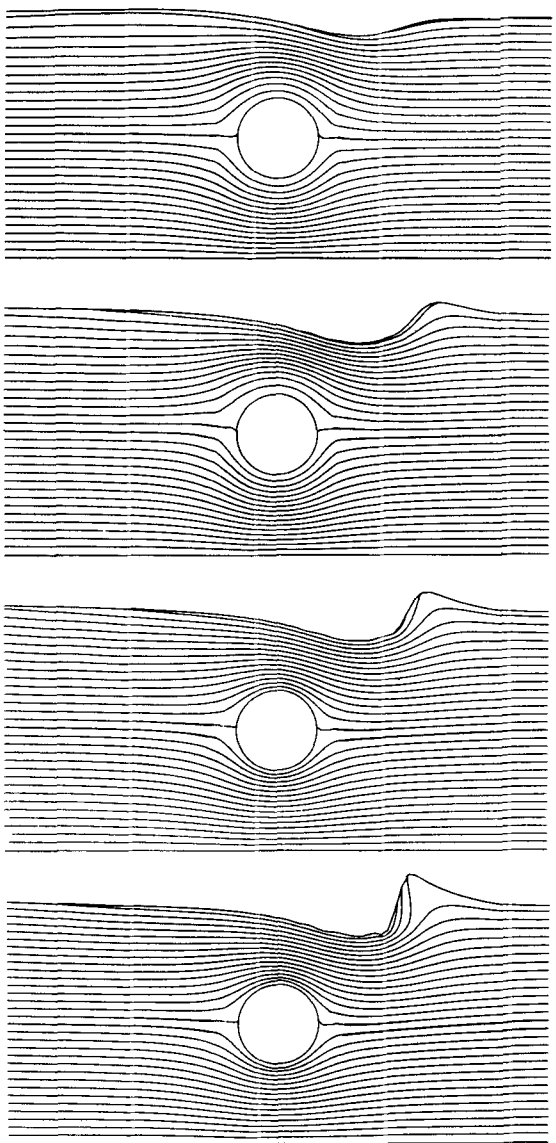

FIGURE 10. Streamlines for $h = 1{\cdot}5$ and $d = 3$. (*a*) $t = 3{\cdot}0$. (*b*) $t = 4{\cdot}8$. (*c*) $t = 5{\cdot}4$. (*d*) $t = 6{\cdot}0$.

as a crude parameterization of the breaking process which also serves to remove energy from the basic flow and reduce wave heights.

The free-surface evolution with the surface pressure acting is presented in figure 11. The surface profile has achieved an almost steady state near the body by $t = 7{\cdot}5$. The trough at about $x = 1$ is shifted considerably downstream from its position in the linear solution. Just downstream from the trough the surface rises abruptly to a high wave crest. The maximum surface slope at $t = 7{\cdot}5$ is $dY/dx \simeq 1{\cdot}5$. The boundary-fitted co-ordinate system at $t = 7{\cdot}5$ is shown in figure 12. A detailed comparison of the surface profile with the pressure applied and the profile with no surface pressure is presented in figure 13. At $t = 4{\cdot}8$ the maximum slope has just exceeded unity, the

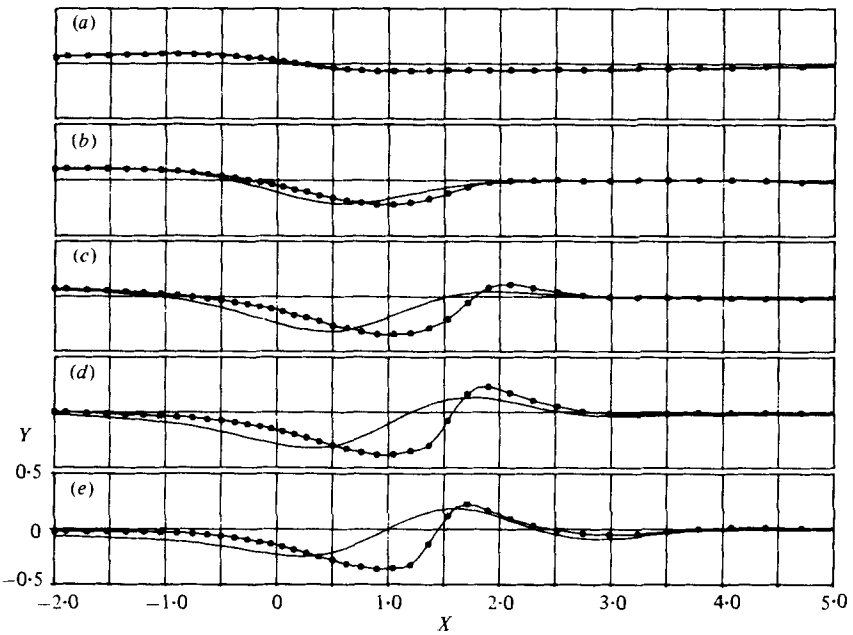

FIGURE 11. Nonlinear free-surface evolution with the surface pressure distribution applied compared with the linear development: $h = 1{\cdot}5$, $d = 3$. ——, linear; —●—, nonlinear. (*a*) $t = 1{\cdot}5$. (*b*) $t = 3{\cdot}0$. (*c*) $t = 4{\cdot}5$. (*d*) $t = 6{\cdot}0$. (*e*) $t = 7{\cdot}5$.

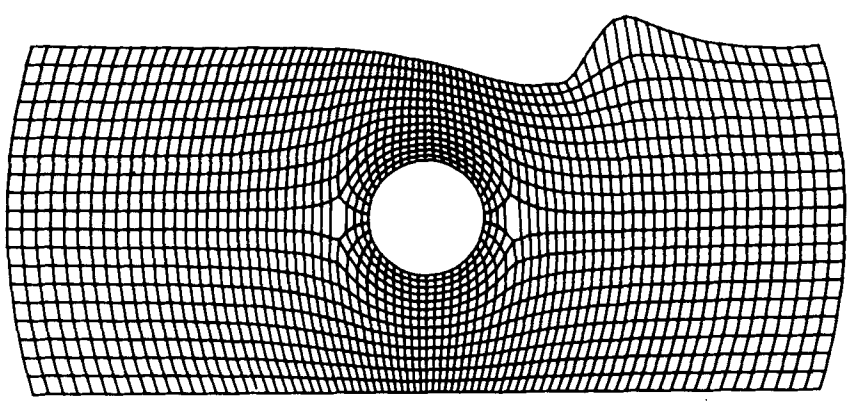

FIGURE 12. The computational co-ordinate system corresponding to figure 11(*e*).

applied pressure is quite small, and the two profiles agree quite closely. By $t = 5{\cdot}4$, more pressure is applied and the profiles begin to deviate more. The comparison at $t = 6{\cdot}0$ is made at the last time at which the results without the surface pressure are available. The approach to steady state beyond $t = 6{\cdot}0$ consists mainly of a gradual upstream movement of the wave with a corresponding upstream shift of the applied surface pressure.

A comparison of the pressure on the cylinder at $t = 6{\cdot}0$ with and without the free-surface pressure is made in figure 14. At least at this time the body surface pressure is essentially independent of the treatment of the free surface on the face of the developing wave. The computed pressure on the body at $t = 7{\cdot}5$ with the free-surface

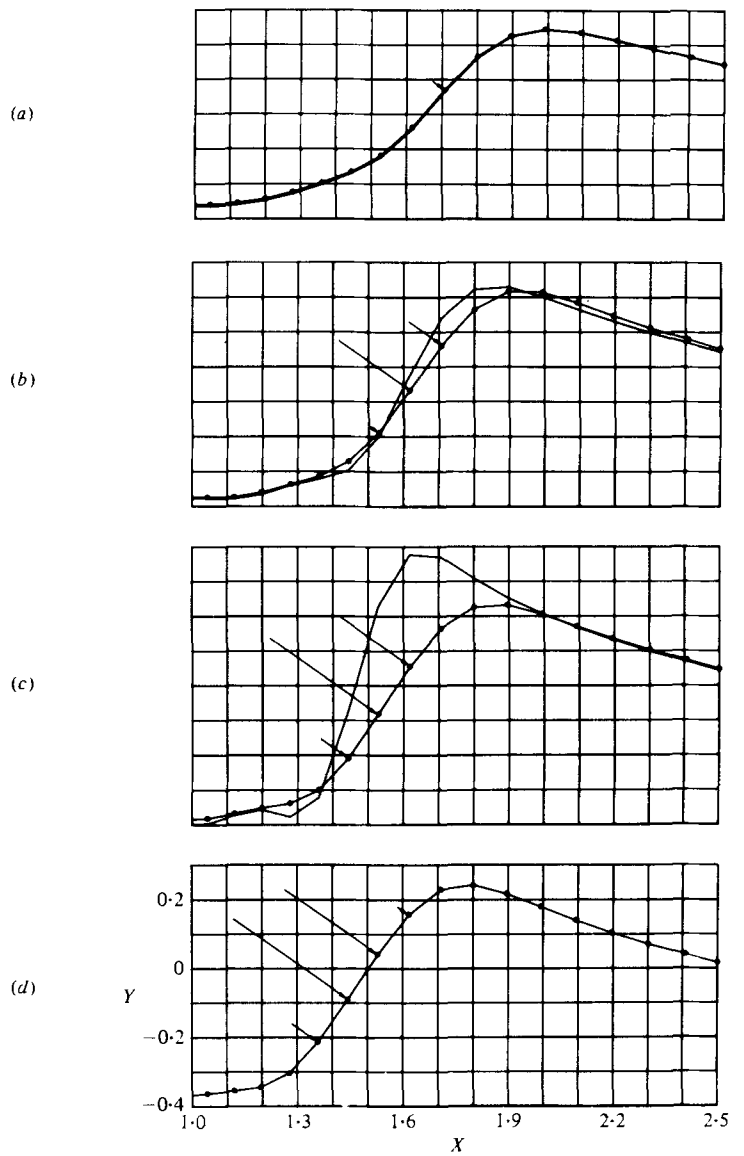

FIGURE 13. The wave development with and without the surface pressure. The lengths of the arrows indicate the strength of the applied pressure. —●—, with pressure; ——, without pressure. (*a*) $t = 4{\cdot}8$. (*b*) $t = 5{\cdot}4$. (*c*) $t = 6{\cdot}0$. (*d*) $t = 6{\cdot}6$.

pressure applied is compared with the steady-state linear body pressure in figure 15. The pressure is significantly lower in the nonlinear case on both the lower and upper surfaces. The nonlinear effects yield a larger pressure difference between the upper and lower surfaces and hence a larger lift. The lift coefficients for the nonlinear and linear cases corresponding to the pressure distributions of figure 15 are $L = 0{\cdot}07$ and $0{\cdot}047$, respectively. The pressure minimum on the upper surface is shifted downstream by the nonlinear effects, reflecting the fact that the narrowest part of the gap between the cylinder and the surface is somewhat downstream from the centre of the body.

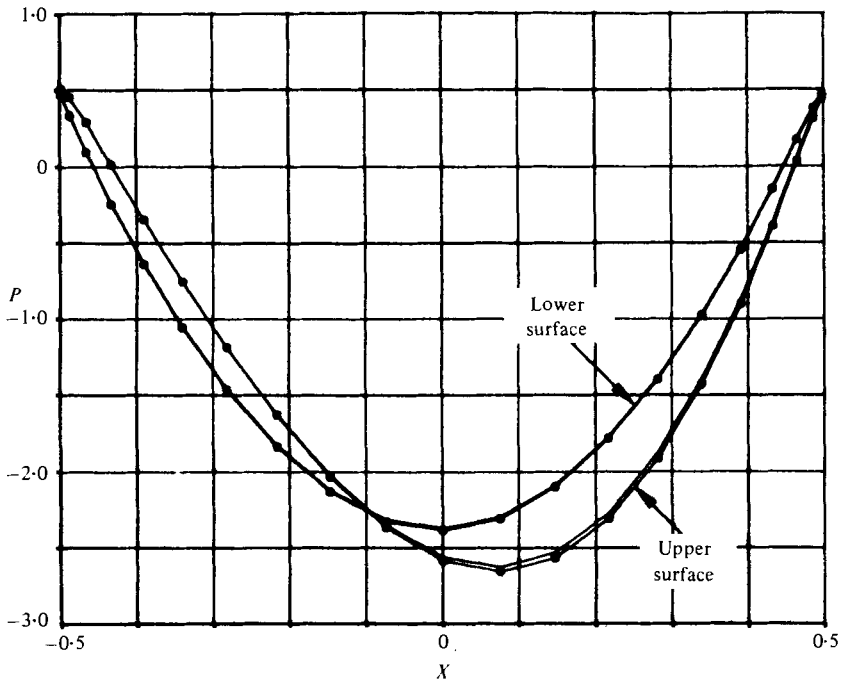

FIGURE 14. The nonlinear dynamic pressure on the body surface at $t = 6$ with and without the pressure applied to the free surface: $h = 1{\cdot}5$, $d = 3$. —●—, with pressure; ——, without pressure.

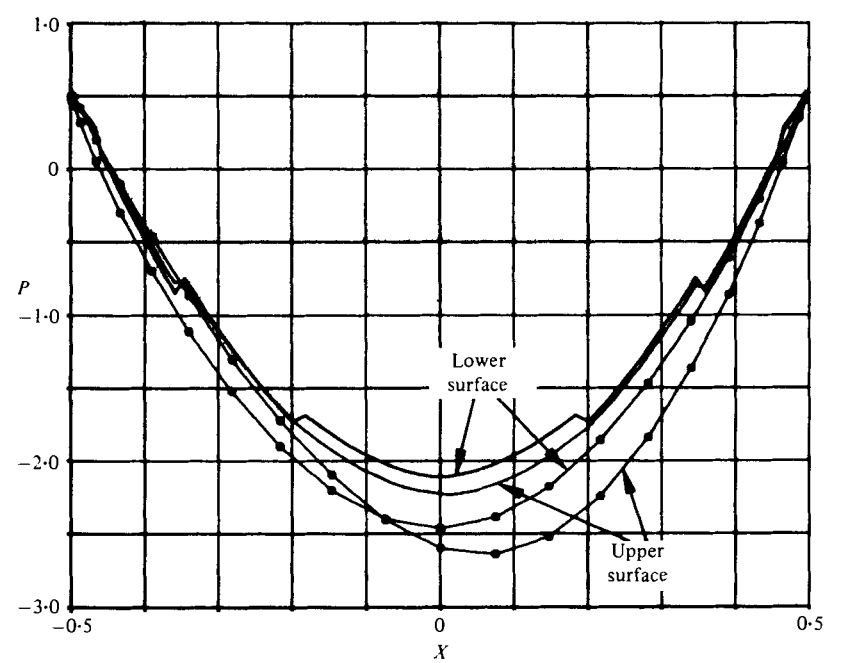

FIGURE 15. The nonlinear dynamic pressure on the body surface corresponding to figure 11 (*d*) compared with the linear steady-state result. ——, linear; —●—, nonlinear.

This downstream shift of the pressure minimum leads to an increase in resistance from $R = 0{\cdot}009$ for the linear case to $R = 0{\cdot}1$ for the nonlinear case.

4.4. $h = 1{\cdot}25$

The free-surface time development was presented in Haussling & Coleman (1977). The evolution was much the same as for $h = 1{\cdot}5$, except that a steep wave slope developed much more rapidly in this case. At $t = 4{\cdot}8$ the maximum slope was

$$dY/dx \simeq 3{\cdot}3$$

and the solution could not be continued further in time. The position and height of the developing wave at $t = 4{\cdot}8$ were about the same as for $h = 1{\cdot}5$ at $t = 6{\cdot}0$.

5. Summary

The results discussed in the previous section illustrate the transition from deep submergence when nonlinear free-surface effects are negligible to shallow submergence when linearized analysis is inaccurate. For submergence depth $h = 2{\cdot}0$ the nonlinear terms are already significant. They lead to a steady-state free-surface elevation having a much higher peak just downstream from the cylinder than is found in the linearized case. For $h = 1{\cdot}5$ a very steep wave slope develops by $t = 6{\cdot}0$. The computations cannot be continued to steady state unless a pressure is applied to the surface to prevent (or simulate) wave breaking. For $h = 1{\cdot}25$ such a steep wave slope appears, and the computations must be terminated even earlier at $t = 4{\cdot}8$. For $h = 1{\cdot}0$ large velocity gradients develop quite early in the calculations and the solution is halted at $t = 0{\cdot}8$. Water flows at high speed through the narrow gap between the cylinder and the free surface at shallow submergence depths. This leads to a low pressure on the upper downstream quadrant of the cylinder and hence higher lift and drag than predicted by the linearized analysis.

The authors acknowledge with gratitude the contribution of Dr P. R. Zarda and Mr M. Marcus who provided some of the linear steady-state solutions. This work was supported by the Numerical Naval Hydrodynamics Programme at the David W. Taylor Naval Ship Research and Development Center. This programme is sponsored jointly by DTNSRDC and the Office of Naval Research.

REFERENCES

Bai, K. J. 1975 A localized finite-element method for steady two-dimensional free-surface flow probelms. *Proc. 1st Int. Conf. Numerical Ship Hydrodyn.*, p. 209. David W. Taylor. Naval Ship Research and Development Center.

Giesing, J. P. & Smith, A. M. O. 1967 Potential flow about two-dimensional hydrofoils. *J. Fluid Mech.* **28**, 113.

Haussling, H. J. & Coleman, R. M. 1977 Finite-difference computations using boundary-fitted co-ordinates for free-surface potential flows generated by submerged bodies. *Proc. 2nd Int. Conf. Numerical Ship Hydrodyn.* University of California at Berkeley.

Havelock, T. H. 1936 The forces on a circular cylinder submerged in a uniform stream. *Proc. Roy. Soc.* A **157**, 526.

Longuet-Higgins, M. S. & Cokelet, E. D. 1976 The deformation of steep surface waves. I. A numerical method of computation. *Proc. Roy. Soc.* A **350**, 1.

MEI, C. C. & CHEN, H. S. 1976 A hybrid element method for steady linearized free-surface flows. *Int. J. Num. Meth. Eng.* **10**, 1153.

SHAPIRO, R. 1975 Linear filtering. *Math. Comp.* **29**, 1094.

THAMES, F. C., THOMPSON, J. F., MASTIN, C. W. & WALKER, R. L. 1977 Numerical solution for viscous and potential flow about arbitrary two-dimensional bodies using body-fitted co-ordinate systems. *J. Comp. Phys.* **24**, 245.

ZARDA, P. R. & MARCUS, M. S. 1977 Finite element solutions of free surface flows. *6th NASTRAN Users' Coll. N.A.S.A. Conf. Publ.* 2018, p. 27.